Molecular Imaging
Volume 15 : 1-9

DOI: 10.1177/1536012116667327
mix.sagepub.com
SAGE

A Novel Copolymer-Based Functional SPECT/MR Imaging Agent for Asialoglycoprotein Receptor Targeting

Pu Zhang, MS[1,2], Zhide Guo, MS[1], Deliang Zhang, MS[1], Chang Liu, MS[2], Guibing Chen, MM[3], Rongqiang Zhuang, PhD[1], Manli Song, MS[1], Hua Wu, PhD[3], and Xianzhong Zhang, PhD[1]

Abstract

The aim of this study is to develop a copolymer-based single-photon emission computed tomography/magnetic resonance (SPECT/MR) dual-modality imaging agent that can be labeled with both technetium-99m (^{99m}Tc) and gadolinium (Gd) and target asialoglycoprotein receptor (ASGPR) via galactose. Monomers of *N*-*p*-vinylbenzyl-6-(2-(4-dimethylamino)benzaldehydehydrazono) nicotinate (VNI) for labeling of ^{99m}Tc, 5,8-*bis*(carboxymethyl)-3-oxo-11-(2-oxo-2-((4-vinylbenzyl)amino)ethyl)-1-(4-vinylphenzyl)-2,5,8,11-tetraazatridecan-13-oic acid (V_2DTPA) for labeling of Gd, and vinylbenzyl-*O*-β-D-galactopyranosyl-D-gluconamide (VLA) for targeting ASGPR were synthesized, respectively. Then the copolymer P(VLA-co-VNI-co-V_2DTPA) (pVLND$_2$) was synthesized and characterized by gel permeation chromatography, dynamic light scattering, and high-performance liquid chromatography analysis. After labeling with ^{99m}Tc and Gd simultaneously, the radiochemical purity, toxicity, relaxivity (r_1), and in vivo SPECT/MR imaging in mice were evaluated. Single-photon emission computed tomography/magnetic resonance imaging and biodistribution results showed that pVLND$_2$ could target ASGPR well. The significantly improved signal to noise ratio was observed in mice liver during MR imaging. All the results suggest that this novel kind of copolymer has the potential to be further developed as a functional SPECT/MR imaging agent.

Keywords

SPECT/MR imaging agent, dual modality, copolymer, molecular imaging, hepatic asialoglycoprotein receptor

Introduction

The hybrid imaging machines that combine single-photon emission computed tomography (SPECT) and computed tomography (CT) or magnetic resonance (MR) imaging modalities together have caused a revolution in the diagnostic imaging.[1-3] Compared to the rapid development of the multimodal instrument, the development of the multimodal probes is slightly lagging behind and the problems cannot be solved by simply adding together 2 different classes of imaging probes unless they happen to have identical pharmacodynamics properties.[4] Therefore, we focused our study on the development of a novel kind of multifunctional agent that could be used for SPECT and MR imaging simultaneously.

In recent years, most studies of the multimodal probes focus on the multifunctional nanoparticles.[5] The combination of 2 or 3 of MR, optical, and radionuclide imaging probe together has been most frequently used as multimodal imaging agents. For example, as early as 2008, Lee et al developed 1 kind of iron-oxide (IO)-based nanoparticle for simultaneous dual MR and positron emission tomography (PET) imaging of tumor intergrin expression.[6] Recently, they also developed one ^{64}Cu-doped chelator-free gold nanoparticle for PET and near-infrared optical imaging.[7] Zhou et al developed a trimodal upconversion luminescence/fluorescence/PET imaging agent

[1] Center for Molecular Imaging and Translational Medicine, State Key Laboratory of Molecular Vaccinology and Molecular Diagnostics, School of Public Health, Xiamen University, Xiamen, China
[2] Key Laboratory of Radiopharmaceuticals, Ministry of Education, College of Chemistry, Beijing Normal University, Beijing, China
[3] Department of Nuclear Medicine, The First Affiliated Hospital of Xiamen University, Xiamen, China

Submitted: 24/03/2015. Revised: 18/10/2015. Accepted: 24/07/2016.

Corresponding Author:
Xianzhong Zhang, School of Public Health, Xiamen University, Xiang'an South Rd., Xiang'an District, Xiamen 361102, China.
E-mail: zhangxzh@xmu.edu.cn

using multifunctional rare earth self-assembled nanosystem.[8] Although nanoparticles have its own advantages for multimodal imaging, there are also many issues like toxicity, biocompatibility, in vivo targeting efficacy, and stability that need to be addressed.[9]

Biocompatible and water-soluble polymers have been used as a platform for drug delivery and molecular imaging for a long time. They have demonstrated unique pharmacokinetic properties such as prolonged blood circulation and tissue retention.[10] In consideration of the advantages of the polymer, we designed and synthesized a copolymer-based functional biomaterial for SPECT/MR imaging. Monomers used for targeting asialoglycoprotein receptor (ASGPR), and for labeling of technetium-99m (^{99m}Tc) and gadolinium (Gd) were synthesized first, then copolymer P(VLA-co-VNI-co-V_2DTPA) (pVLND$_2$) was synthesized by radical copolymerization reaction. Compared with the rigid globular nanoparticles, it was necessary to synthesize a liner flexible copolymer to combine with the target position more tightly and efficiently, and the composition of the copolymer can be adjusted by changing the ratio of the monomers.

The ASGPR[11] is well known, existing on the surface of normal hepatocyte membrane[12] and participating in the binding, internalization, and subsequent clearance from the circulating glycoproteins that contain terminal galactose or *N*-acetylglucosamine (GlcNAc) residues through Ca^{2+}-dependent endocytosis and lysosomal degradation.[13-16] Previous studies have demonstrated that the number of ASGPR could reflect the degree of various liver diseases, such as hepatitis and cirrhosis[17]; so the ASGPR is considered as an attractive molecular target for diagnostic imaging. The ASGPR imaging agents, such as ^{99m}Tc-LSA,[18] ^{99m}Tc-DTPA-LSA,[19] ^{99m}Tc-NGA,[20,21] ^{99m}Tc-DMP-NGA,[22] [^{18}F]FNGA,[23] ^{99m}Tc-DTPA-galactosyl human serum albumin (GSA),[24] and so on, carrying galactose as targeted molecule have been studied and developed extensively during these years. Yang et al had developed 1 kind of copolymer-based ASGPR targeting agent for SPECT imaging before, both of them showed excellent liver targeting properties.[25,26] With ASGPR as an excellent hepatic target, we now try to synthesize 1 multifunctional agent that can target ASGPR to evaluate the function and status of liver.

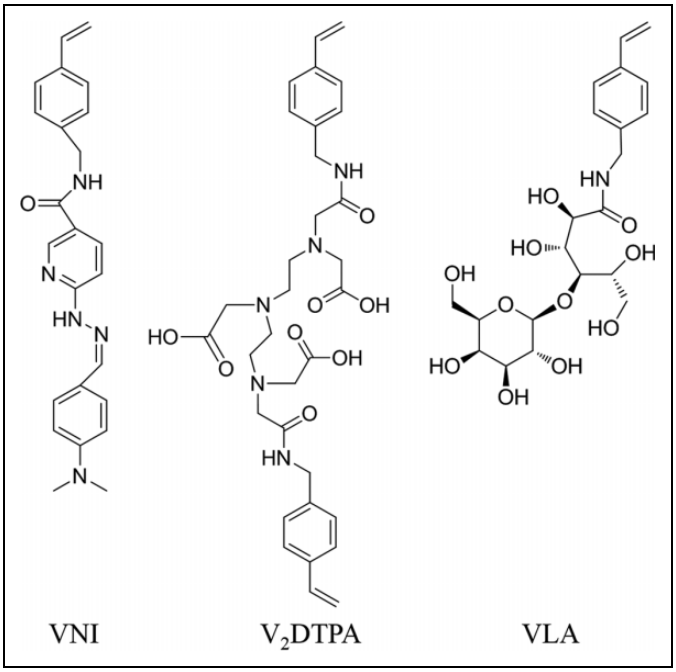

Figure 1. Structure of 3 monomers: VNI for labeling of ^{99m}Tc; V_2DTPA for labeling of Gd; and VLA for targeting ASGPR. ^{99m}Tc indicates technetium-99m; ASGPR, asialoglycoprotein receptor; Gd, gadolinium; V_2DTPA, 5,8-*bis*(carboxymethyl)-3-oxo-11-(2-oxo-2-((4-vinylbenzyl)amino)ethyl)-1-(4-vinylphenzyl)-2,5,8,11-tetraazatridecan-13-oic acid; VLA, vinylbenzyl-*O*-β-D-galactopyranosyl-D-gluconamide; VNI, *N*-*p*-vinylbenzyl-6-(2-(4-dimethylamino)benzaldehydehydrazono) nicotinate.

Materials and Methods

Materials

The 4-Vinylbenzyl chloride, phthalimide potassium derivative, hydrazine hydrate, 6-chloronicotinic acid, anhydrous dimethylsulfoxide (DMSO) were purchased from Acros Organics (New Jersey). The 4-Dimethylaminobenzaldehyde, *N*-hydroxysuccinimide, dicyclohexylcarbodiimide, and Tin(II) chloride (anhydrous) were purchased from J&K (Beijing, China). Gadolinium(III) chloride was purchased from REO (Newburyport, Massachusetts). Acetonitrile was purchased from Burdick&-Jackson (Ulsan, Korea). *N*,*N*-Dimethylformamide (DMF) and ethanol (95%) were purchased from Sinopharm Chemical Reagent Co., Ltd (Beijing, China). Trifluoroacetic acid (TFA) was purchased from Aladdin Industrial Inc (Shanghai, China). C57BL/6 mice (female, 6 weeks) and ICR mice (female, 8 weeks) were obtained from Laboratory Animal Center of Xiamen University (Xiamen, China). All in vivo animal procedures were approved by the Institutional Animal Care and Use Committee of Xiamen University.

Synthesis of Monomer V_2DTPA

The monomers *N*-*p*-vinylbenzyl-6-(2-(4-dimethylamino)benzaldehydehydrazono) nicotinate (VNI) and vinylbenzyl-*O*-β-D-galactopyranosyl-D-gluconamide (VLA) (Figure 1) were prepared according to the procedure reported previously.[26] The *p*-vinylbenzylamine (VBA) was prepared from 4-vinylbenzyl chloride according to the Gabriel synthesis[27] for the synthesis of monomer 5,8-*bis*(carboxymethyl)-3-oxo-11-(2-oxo-2-((4-vinylbenzyl)amino)ethyl)-1-(4-vinylphenzyl)-2,5,8,11-tetraazatridecan-13-oic acid (V_2DTPA; Figure 1). Briefly, 0.5 mL triethylamine was added to 1.5 mmol VBA (0.2 g, dissolved in 2 mL anhydrous DMF), then 1.5 mmol diethylenetriaminepentaacetic dianhydride (0.536 g, dissolved in 2 mL anhydrous DMF) was added. The solution was stirred under N_2 at room temperature for 30 hours. After the solvent DMF was removed through evaporation, 10 mL water was added and the pH of the solution was adjusted to 10 to obtain the settled solution. Then the solution was washed twice with 5 mL ether, the pH was

adjusted to 5 and then filtrated to obtain the monomer V_2DTPA. It was dried under high-vacuum condition and stored as a powder. The 3 monomers were all identified by proton nuclear magnetic resonance (NMR) and mass spectrum analysis.

Syntheses of Copolymers P(VNI-co-V_2DTPA) and P(VLA-co-VNI-co-V_2DTPA)

The mixture of VNI and V_2DTPA was dissolved in anhydrous DMSO with the molar ratio of 1:4 and the azobisisobutyronitrile was added as an initiator. The mixture was stirred for 24 hours at 60°C. After polymerization, the solution that contained the copolymer was dialyzed against DMSO for 3 days, phosphate buffer (pH 7.4, 0.05 mol/L) for 1 day, and finally deionized water for another 3 days (molecular weight cutoff, 2 kDa). The resulting solution was lyophilized to obtain the product P(VNI-co-V_2DTPA) (pVND$_2$). The copolymer P(VLA-co-VNI-co-V_2DTPA), in short pVLND$_2$, which contained the targeting monomer VLA, was synthesized similarly, except that the molar ratio of VLA, VNI, and V_2DTPA was adjusted to 5:1:4.

Synthesis of Gadolinium-Labeled p$VLND_2$

Ten milligram pVLND$_2$ (dissolved in 1 mL water) were added dropwise to 20 mg $GdCl_3$ solution (in 1 mL water) under stirring. After stirring for 24 hours at room temperature, the solution was dialyzed against deionized water for 3 days to remove the unlabeled Gd^{3+}. The resulting solution was lyophilized to obtain the product Gd-pVLND$_2$.

Characterization of Copolymers

The molecular weight distribution analysis of copolymers (pVND$_2$, pVLND$_2$) was performed by size exclusion chromatography. The chromatograms were collected on a TSKgel (G4000PWxl) column at 254 nm wavelength, with water (1% TFA) as the mobile phase. Dynamic light scattering (DLS) was applied to determine the hydrodynamic diameter of the copolymers and zeta potential was also measured on the Malvern Zetasizer Nano ZS90 (Malvern, UK). The purity of the copolymers was performed by high-performance liquid chromatography (HPLC) analysis. The chromatograms were collected on a Nucleosil (Macherey-Nagel, Germany) C18 (250 × 4 mm, 10 μm, 100 Å) at 254 nm wavelength, with acetonitrile and water as the mobile phase. The gradient condition was 0 to 9 minutes, 30% acetonitrile (1% TFA) and 9 to 20 minutes, 50% acetonitrile (1% TFA). The flow rate was 1 mL/min. The percentage composition of galactose in the copolymer pVLND$_2$ was determined using phenol-concentrated sulfuric acid method and NMR spectrum analysis. The content of Gd in Gd-pVLND$_2$ was analyzed by inductively coupled plasma mass spectrometry (ICP-MS).

Synthesis of ^{99m}Tc-Labeled Copolymers

One milligram copolymer (pVND$_2$ or Gd-pVLND$_2$) was weighed in a 10-mL vial; then 0.6 mL phosphate buffer (pH 7.4, 0.05 mol/L), 15 μL $SnCl_2$ solution (3 mg/mL in 1 mol/L HCl), and 0.3 mL freshly eluted $Na^{99m}TcO_4$ (~148-185 MBq) from a commercial generator were added into the vial successively. The vial was sealed and heated for 30 minutes at 60°C. The labeling yield was detected by instant thin-layer chromatography–silica gel/acid citrate/dextrose (ITLC-SG/ACD; citrate–glucose buffer solution, citrate [0.068 mol/L], glucose [0.074 mol/L], pH 5.0).

Octanol–Water Partition Coefficient

To determine the hydrophilicity of the radiolabeled copolymers, 3.7 MBq tracer was diluted in 3 mL phosphate-buffered saline (PBS; 0.05 mol/L, pH 7.4) and added equal volume of 1-octanol. After vigorous mixing for 5 minutes, the mixture was separated by centrifugation for 5 minutes with 8000 rpm. A 100 μL aqueous solution was taken out and added into the mixture of PBS (2.9 mL) and 1-octanol (3 mL) for another vortex mixing and centrifugation. Once again the procedure was repeated. Counts of 100 μL organic and 100 μL aqueous phase ($n = 3$) were determined by γ-counter (Wizard 2480; Perkin Elmer, Massachusetts, USA). The log P value was reported as mean ± SD of 3 independent measurements.

Stability of ^{99m}Tc-Labeled Gd-p$VLND_2$

^{99m}Tc-Gd-pVLND$_2$ (about 1.85 MBq) was incubated in saline and fresh serum of ICR mice at 37°C for 4 hours. Then 200 μL of acetonitrile was added into the serum, centrifuged at 5000 rpm for 5 minutes at 4°C and the supernatant was collected. After that the solution of the saline and the supernatant were passed through 0.22-μm Millipore filter and analyzed by HPLC.

Measuring Relaxivity r_1 of Gd-p$VLND_2$

The T_1 relaxation time of Gd-pVLND$_2$ and Magnevist (Gd-DTPA) at different concentrations were measured in test tubes on a 9.4 T animal MR imaging scanner (BioSpec 94/20USR; Bruker, Germany). The longitudinal (r_1) relativity was calculated from $r_1 = (1/T_1 - 1/T_0)/c$, where c is the concentration of Gd^{3+}, T_1 is the relaxation time at concentration c, and T_0 is the relaxation time of water.

Methyl Thiazolyl Tetrazolium Assay

Cytotoxicity in vitro was measured by the methyl thiazolyl tetrazolium (MTT) assay using the LO2 cell line. The cells were seeded into a 96-well culture plate with a density of 1×10^4 cells/well in Dulbecco's-modified eagle medium (DMEM) with 10% fetal bovine serum at 37°C and 5% CO_2 for 24 hours. Then the cells were incubated with the copolymers pVLND$_2$ and Gd-pVLND$_2$, respectively, at different concentrations (0, 200, 400, 800, 1000 μg/mL in DMEM) for 24 hours at 37°C and 5% CO_2. Thereafter, MTT (10 μL, 5 mg/mL) was added to each well and the plates were incubated for additional 4 hours at 37°C under 5% CO_2. A scientific

microplate reader (Multiskan Spectrum; Thermo Fisher, USA) was used to measure the optical density (OD; absolute value at 490 nm) of each well, with background subtraction at 690 nm.

Establishment of Hepatic Fibrosis Mice Model

Six-week-old female C57BL/6 mice were treated with 0.1 mL CCl_4 solution (20% in olive oil) twice a week by intraperitoneal injection for 4 weeks to establish the hepatic fibrosis mice model. To demonstrate the successful establishment of hepatic fibrosis mice model, the histology study was performed. Specimens were fixed in 10% buffered formalin and embedded in paraffin. Serial sections (5 μm) were cut and stained with hematoxylin and eosin (H&E) and Sirius red staining.

Biodistribution

The tissue distribution characteristics of ^{99m}Tc-Gd-*p*VLND$_2$ were performed using normal ICR mice. About 0.185 MBq ^{99m}Tc-Gd-*p*VLND$_2$ (in 100 μL solution) was injected into the mice through the tail vein. At 5, 30, 60, 120, and 240 minutes after injection, mice (n = 5 at each time point) were killed, and the tissues and organs of interest were collected, wet weighted, and counted in a γ-counter. The percentage injected dose per gram (% ID/g) for each sample was calculated by comparing its activity with an appropriate standard of ID. The blocking study was performed by co-injecting the tracer with 200 μg GSA or cold copolymer into the mice and killed the mice (n = 5) 5 minutes after injection.

In Vivo SPECT Imaging

Single-photon emission computed tomography/magnetic resonance /CT images of mice were acquired using nanoScan SC (Mediso Medical Imaging System, Budapest, Hungary) equipped with pinhole collimator under standard animal scan procedure. The following parameters were obtained: energy peak of 50 kV, 670 μA, 480 projections, medium zoom, and 50 seconds/frame. 8-week-old female normal ICR mice and hepatic fibrosis C57BL/6 mice were used to perform SPECT/CT imaging. While imaging, about 18 MBq of ^{99m}Tc-Gd-*p*VLND$_2$ was injected into the mouse intravenously.

The MR Imaging of Gd-pVLND$_2$

Both Gd-*p*VLND$_2$ and Magnevist (Gd^{3+}, 0.1 mmol/kg) were intravenously injected into the normal ICR mice at the same concentration of Gd^{3+}. T_1-weighted images of the mouse were acquired at different time using a 9.4 T MR imaging scanner (BioSpec 94/20USR). A commercially available volume coil (diameter 40 mm, RF RES 400 ^{1}H 075/040 QSN TR; Bruker, Germany) was used. T_1-weighted Tueborapid acquisition with relaxation enhancement (RARE) images (repetition time [TR] = 1500 ms, echo time [TE] = 8.5 ms, field of view 4 × 4 cm, slice thickness = 1 mm) were acquired from sagittal slice. After scanning, the animals were removed from the magnet and allowed to recover in a warm environment.

Results and Discussion

Synthesis and Characterization of pVND$_2$, pVLND$_2$, and Gd-pVLND$_2$

The absorption, distribution, metabolism, and excretion of the polymer all depend on the physicochemical characteristics, such as molecular weight, solubility, and charge of the polymer.[28] For nuclear medicine and MR imaging, if the tracer or the contrast agent accumulates in the nontargeted organ, it may cause radiation hurt or other side effects. Therefore, the copolymers with appropriate molecular weight and excellent water solubility are needed for polymer-based imaging agents. The copolymers of *p*VND$_2$ with different molecular weight have been synthesized at different concentrations of the 2 monomers VNI and V_2DTPA (Table S1).

Through the size exclusion chromatography analysis of the copolymer *p*VND$_2$ polymerized at 3 different monomer concentrations (Figure 2A-C), we found that the copolymer polymerized in 3 mL DMSO had the most narrow molecular weight distribution. The HPLC ultraviolet (UV) analysis results of the copolymer are shown in Figure 2D-F; their chemistry purity were all over 99%. The octanol–water partition coefficient log P of the copolymer was determined, and the results (Table S1) showed that even though they had similar octanol–water partition coefficient, the copolymer polymerized in 3 mL DMSO had the most excellent water solubility.

Considering the molecular weight distribution and the water solubility of the copolymer *p*VND$_2$, copolymer *p*VLND$_2$ which had galactose as targeting molecule was synthesized at the same monomer concentrations in 3 mL DMSO. The size exclusion chromatography analysis result of *p*VLND$_2$ is shown in Figure 3A, which had the very similar retention time (8.818 min) with the copolymer *p*VND$_2$ (8.820 min), and through the quantitative analysis we know the number-average molecular weight of *p*VLND$_2$ was 5.34×10^3. The DLS analysis of *p*VND$_2$ (Figure 4A) and *p*VLND$_2$ (Figure 4B) confirmed that the 2 kinds of copolymers had a uniform and similar hydrodynamic diameter. The zeta potential of *p*VND$_2$ and *p*VLND$_2$ was, respectively, -42.2 ± 2.5 mV and -34.5 ± 3.3 mV. The sugar density of the copolymer was calculated as 22.95% (m/m) by determining the absorption value of *p*VLND$_2$ at the specific absorption wavelength 490 nm (0.128 ± 0.0006) and according to the standard curve of galactose density (Figure S5). Then we labeled the copolymer *p*VLND$_2$ with Gd. The HPLC results of *p*VLND$_2$ and Gd-*p*VLND$_2$ are shown in Figure 3B, C which indicated the high chemistry purity of the probe. According to the ICP-MS analysis result, it was found that the Gd content of the Gd-*p*VLND$_2$ was 152.735 mg/g.

Synthesis and Stability of ^{99m}Tc-Labeled Gd-pVLND$_2$

High labeling yield of ^{99m}Tc-Gd-*p*VLND$_2$ was obtained under the optimized labeling condition (reaction at pH 7.0 for 30 min at 60°C). The labeling yield determined by ITLC-SG/ACD was

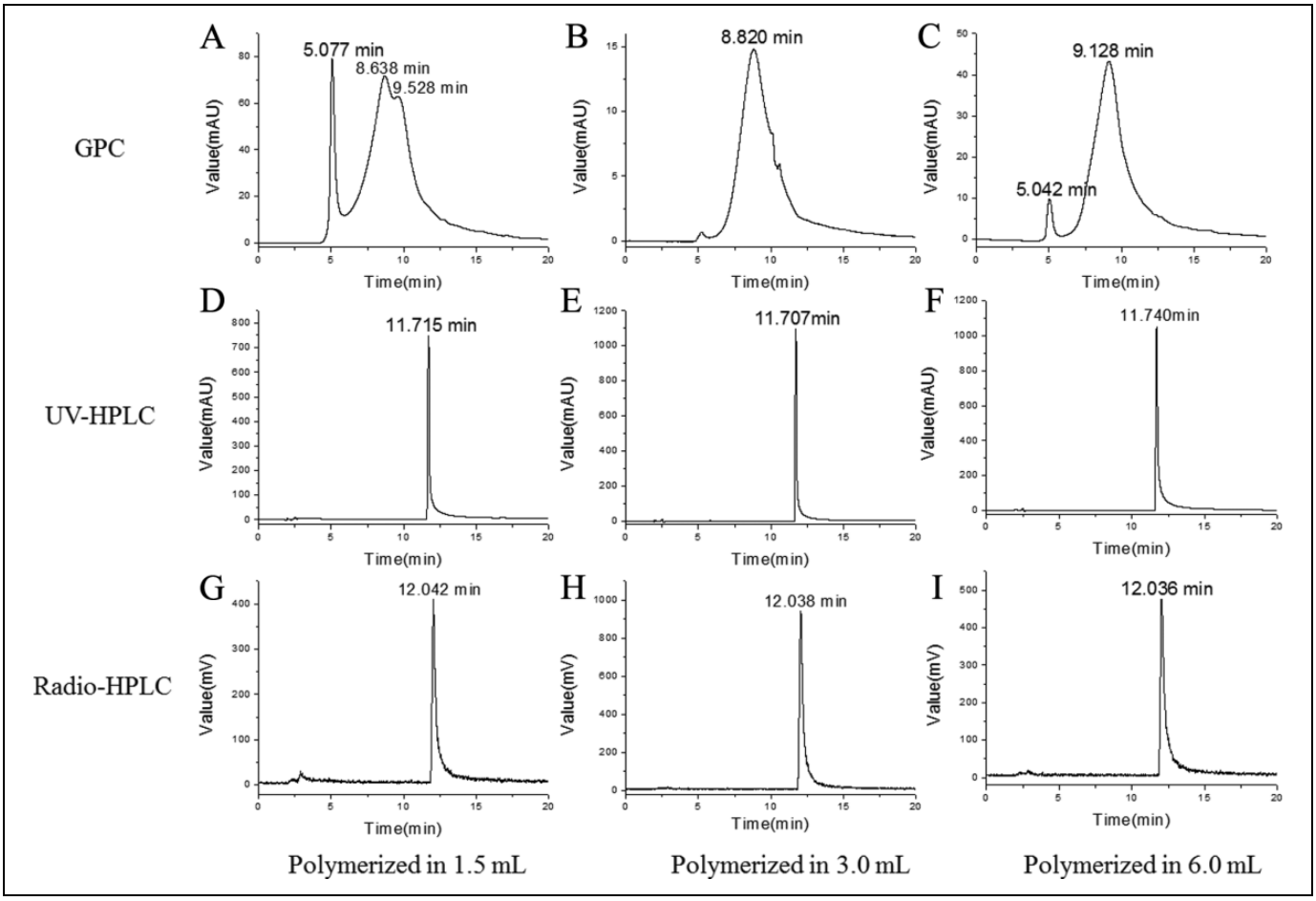

Figure 2. A to C, The GPC analysis of pVND$_2$ (polymerized in 1.5 mL, 3.0 mL, 6.0 mL DMSO, respectively) at 254 nm; D to F, The UV-HPLC analysis of pVND$_2$ (polymerized in 1.5 mL, 3.0 mL, 6.0 mL DMSO, respectively) at 254 nm; G to I, Radio-HPLC analysis of ^{99m}Tc-pVND$_2$ (polymerized in 1.5 mL, 3.0 mL, and 6.0 mL DMSO, respectively). ^{99m}Tc indicates technetium-99m; DMSO, dimethylsulfoxide; GPC, gel permeation chromatography; pVND$_2$, P(VNI-co-V$_2$DTPA); UV-HPLC, ultraviolet-high performance liquid chromatography.

greater than 95%. The complex ^{99m}Tc-Gd-pVLND$_2$ remained at the spotting point (R_f = 0-0.1) while other radioactive impurities like hydrolyzed ^{99m}Tc and $^{99m}TcO_4^-$ moved to the front of the strips (R_f = 0.9-1.0, shown in Figure S6). The HPLC result (Figure 3D) showed that the radiochemical purity of ^{99m}Tc-Gd-pVLND$_2$ was greater than 98% and the retention time was 12.050 minutes. In vitro stability study (Figure 3E, F) showed that after incubating in saline and fresh serum of ICR mice at 37°C for 4 hours, the ^{99m}Tc-Gd-pVLND$_2$ was still intact and the retention times were, respectively, 12.022 minutes and 12.023 minutes, which were consistent with the retention time of Gd-pVLND$_2$.

Magnetic Relaxation Property of Gd-pVLND$_2$

To evaluate the magnetic relaxation property of the Gd-pVLND$_2$, the longitudinal (r_1) relativity of the aqueous solution containing the copolymer at various Gd^{3+} concentrations were measured using a 9.4 T animal MR imaging scanner. Figure 5 shows the MR imaging results of Gd-pVLND$_2$ solution at different concentrations. The longitudinal (r_1) relativity of the Magnevist at different concentrations was also measured. From Figure 5, the r_1 relaxivity of Gd-pVLND$_2$ was calculated as 11.40 M^{-1} s^{-1}, which was higher than that of clinical reagent Magnevist (4.60 M^{-1} s^{-1}).

Cytotoxicity

The MTT assay was performed on human hepatic cell line LO2 to evaluate the in vitro cytotoxicity of Gd-labeled copolymer Gd-pVLND$_2$. The cells were incubated with varying concentrations of copolymers pVLND$_2$ and Gd-pVLND$_2$, respectively, for 24 hours. The viability of cells incubated with copolymer Gd-pVLND$_2$ was a little lower than the viability of cells incubated with copolymer pVLND$_2$, but even in the concentration of 1 mg/mL Gd-pVLND$_2$, the viability was also higher than 90% (Figure 6), so the MTT assay demonstrated that the Gd- labeled copolymer Gd-pVLND$_2$ had low cytotoxicity.

Biodistribution

Normal female ICR mice weighing about 20 g were used to perform the biodistribution study of ^{99m}Tc-labeled copolymer

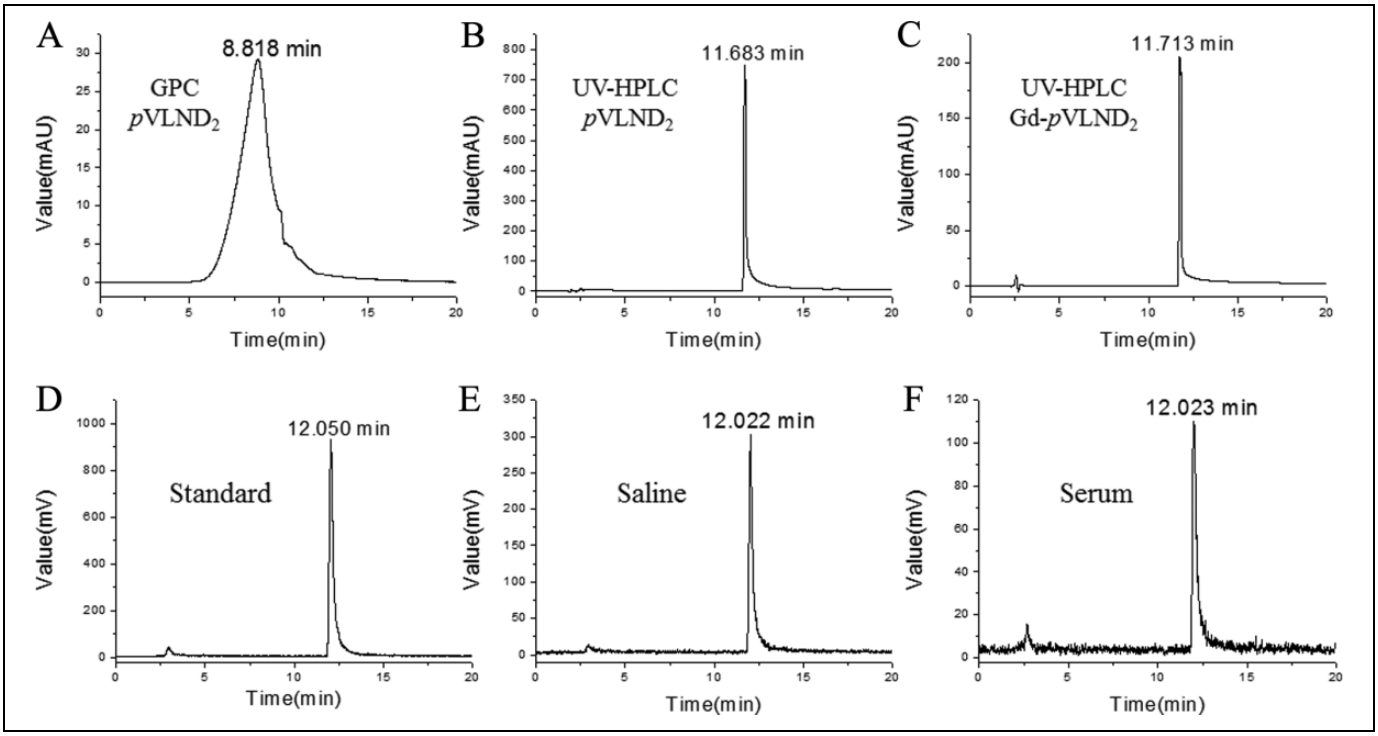

Figure 3. A, The GPC analysis of pVLND$_2$; B, The UV-HPLC analysis of pVLND$_2$ at 254 nm; C, The UV-HPLC analysis of Gd-pVLND$_2$ at 254 nm; D, Radio-HPLC analysis of ^{99m}Tc-Gd-pVLND$_2$; E, Radio-HPLC analysis of ^{99m}Tc-Gd-pVLND$_2$ (incubated in saline at 37°C for 4 hours); F, Radio-HPLC analysis of ^{99m}Tc-Gd-pVLND$_2$ (incubated in serum at 37°C for 4 hours). ^{99m}Tc indicates technetium-99m; Gd, gadolinium; GPC, gel permeation chromatography; pVLND$_2$, P(VNI-co-V$_2$DTPA); UV-HPLC, ultraviolet-high performance liquid chromatography.

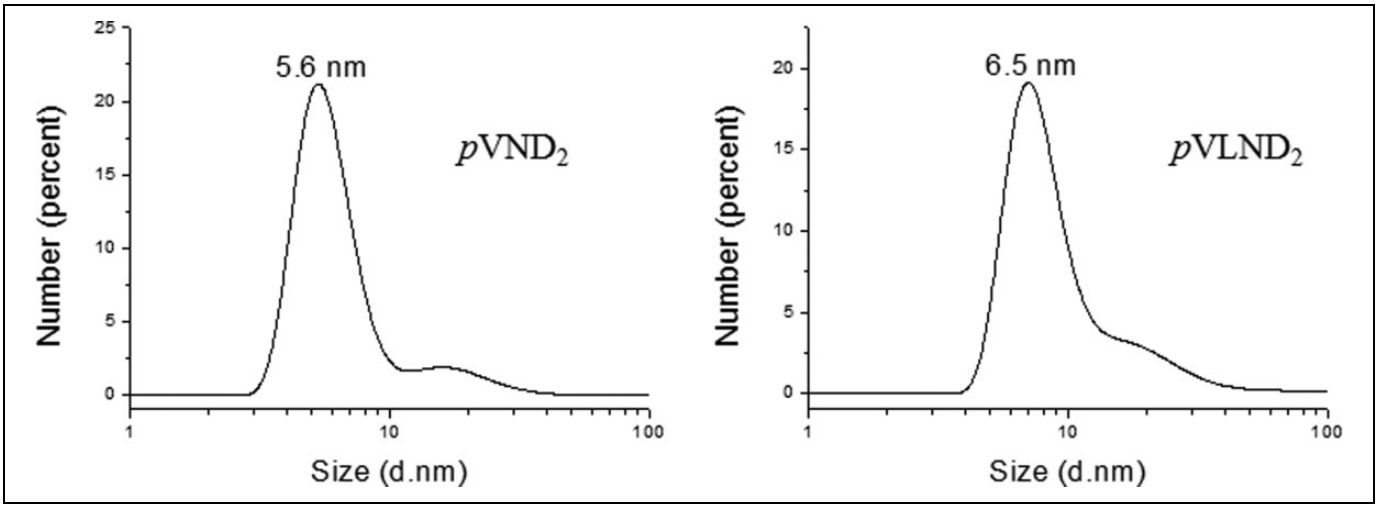

Figure 4. The DLS analysis of copolymers pVND$_2$ and pVLND$_2$. DLS indicates dynamic light scattering; pVLND$_2$, P(VLA-co-VNI-co-V$_2$DTPA); pVND$_2$, P(VNI-co-V$_2$DTPA).

Gd-pVLND$_2$. In Figure 7, very high liver accumulation was sustained for up to 240 minutes after injection, while low uptakes were found in other organs or tissues. The liver uptake was 79.50 $\pm$ 6.01 %ID/g at 5 minutes after injection, then decreased to 50.47 $\pm$ 5.31 %ID/g at 240 minutes after injection (Table S2). In the blocking studies, the liver uptake decreased apparently from 79.50 $\pm$ 6.01 %ID/g to 43.78 $\pm$ 2.98 %ID/g by using cold GSA as the blocking agent; while using cold copolymer pVLND$_2$ as the blocking agent, the liver uptake was significantly decreased to 12.96 $\pm$ 1.14 %ID/g (Table S2). Different blocking efficacies were found for GSA and pVLND$_2$, which agreed well with our previously published literature.[26] The reason may be due to the nonspecific binding of ^{99m}Tc-Gd-pVLND$_2$ to the liver macrophage, which could only be blocked by its cold copolymer pVLND$_2$.[29]

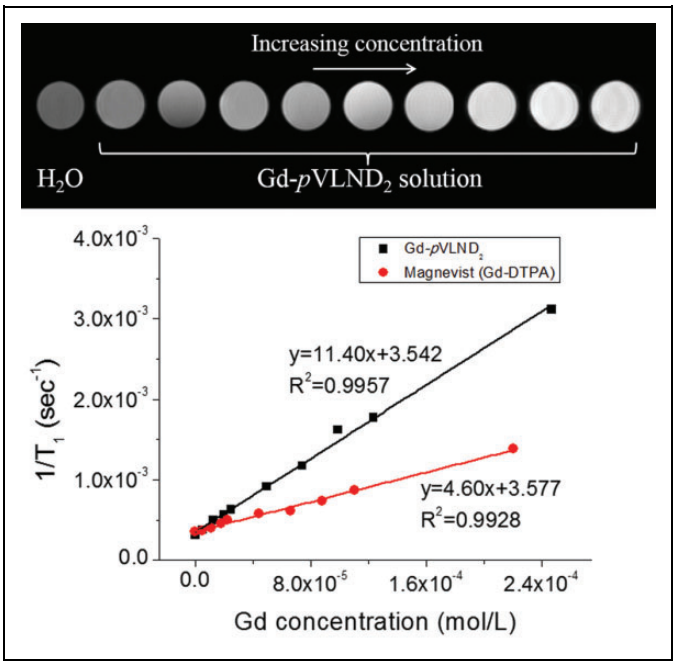

Figure 5. Relaxivity r_1 measurement results of Gd-pVLND$_2$. Gd indicates gadolinium; pVLND$_2$, P(VLA-co-VNI-co-V$_2$DTPA).

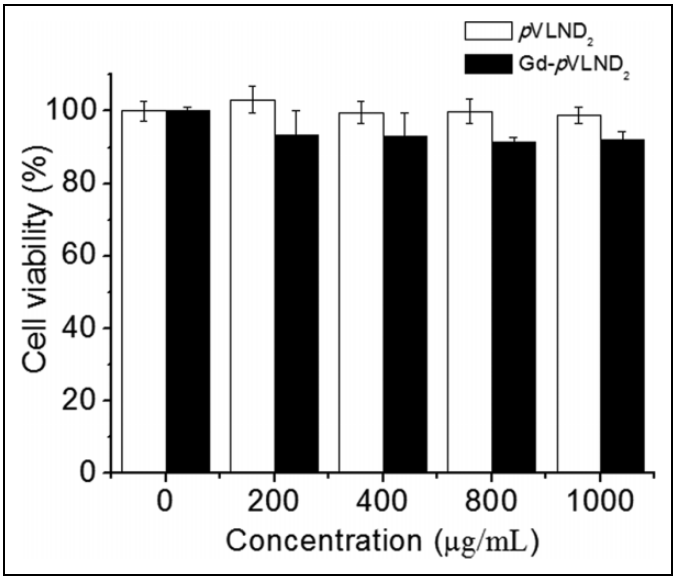

Figure 6. Cell viability values (%) of LO2 cells after 24 hours incubation in DMEM medium with the varying concentrations of pVLND$_2$ and Gd-pVLND$_2$, respectively (n = 3). DMEM indicates Dulbecco's-modified eagle medium; Gd, gadolinium; pVLND$_2$, P(VLA-co-VNI-co-V$_2$DTPA).

The further feasibility studies of ^{99m}Tc-Gd-pVLND$_2$ with SPECT imaging for assessing hepatic function and comparison of it with previously reported imaging agents, such as ^{99m}Tc-GSA[24] and ^{99m}Tc-[P(VLA-co-VNI)](tricine)$_2$[26], will be investigated in the future.

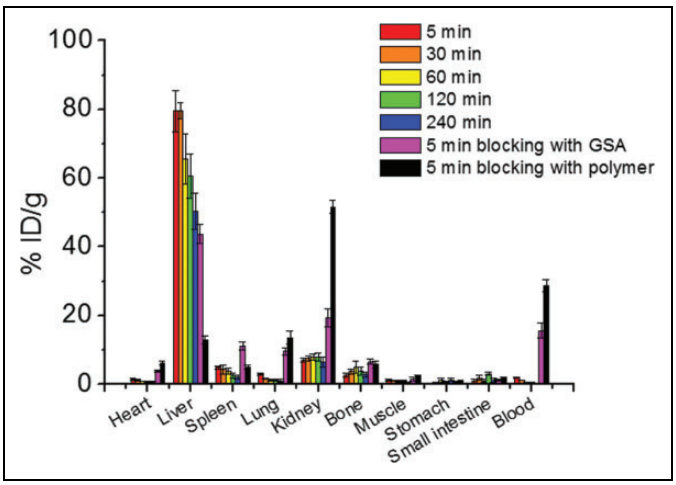

Figure 7. Biodistribution results of ^{99m}Tc-Gd-pVLND$_2$ in mice (n = 5). ^{99m}Tc indicates technetium-99m; Gd, gadolinium; pVLND$_2$, P(VLA-co-VNI-co-V$_2$DTPA).

Single-Photon Emission Computed Tomography/ Magnetic Resonance Imaging

The results of SPECT imaging are shown in Figure 8. Comparing the imaging results of ^{99m}Tc-pVND$_2$ and ^{99m}Tc-Gd-pVLND$_2$ in normal ICR mice at 30 minutes and 1 hour (Figure 8A, B), the uptake of ^{99m}Tc-Gd-pVLND$_2$ was much higher than that of ^{99m}Tc-pVND$_2$ under the condition that injected the same chemical and radioactive quantity into the mice. In the blocking experiment, 400 μg GSA was coinjected with ^{99m}Tc-Gd-pVLND$_2$ into the mice intravenously. In the control group, strong contrast between liver and other untargeted organs was obtained (Figure 8C, D). For the blocking group, visible decreased uptake of the tracer in the liver showed specific binding to the ASGPR (Figure 8C, D). Figure 8E and F shows the results of SPECT imaging of liver fibrosis C57BL/6 mice which was induced by carbon tetrachloride. Comparing with the normal C57BL/6 mice, the liver uptake of the tracer was decreased and uneven in the liver fibrosis mice. Based on the results of SPECT imaging, the radiolabeled copolymer Gd-pVLND$_2$ could rapidly accumulate in the liver of a normal mice and had defected liver uptake in fibrosis mice, which demonstrated the potential ability of the tracer to diagnose some hepatic disease.

The MR Imaging

The MR images of a normal ICR mice are shown in Figure 9. After Gd-pVLND$_2$ injection, the obvious enhancement of T_1 contrast of the liver was found in the normal mice during 30 minutes. The signal to noise ratio of the liver was determined by choosing an appropriate and same region of interest (avoiding the blood vessel) in the mouse liver before and after Gd-pVLND$_2$ injection (Figure S8), and the results indicated that the enhancement at the beginning and 5 minutes after injection were 62% and 52%, respectively. The liver blood vessel also had an obvious T_1 contrast enhancement due to the

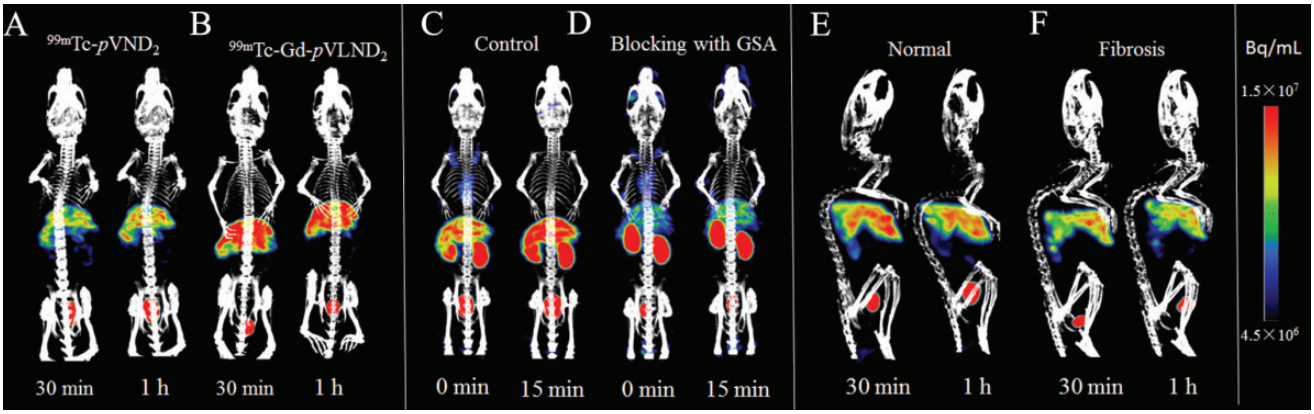

Figure 8. Single-photon emission computed tomography/magnetic resonance (SPECT)/CT images of normal ICR mice at 30 minutes and 1 hour after injection of ^{99m}Tc-pVND$_2$ (A) and ^{99m}Tc-Gd-pVLND$_2$ (B); The SPECT/CT images of normal ICR mice at 0 minutes and 15 minutes after injection of ^{99m}Tc-Gd-pVLND$_2$ (C) and coinjection with 400 μg GSA (D); The SPECT/CT images of normal C57BL/6 mice (E) and hepatic fibrosis C57BL/6 mice (F) at 30 minutes and 1 hour after injection of ^{99m}Tc-Gd-pVLND$_2$. ^{99m}Tc indicates technetium-99m; Gd, gadolinium; GSA, galactosyl human serum albumin; pVLND$_2$, P(VLA-co-VNI-co-V$_2$DTPA); pVND$_2$, P(VNI-co-V$_2$DTPA); CT, computed tomography.

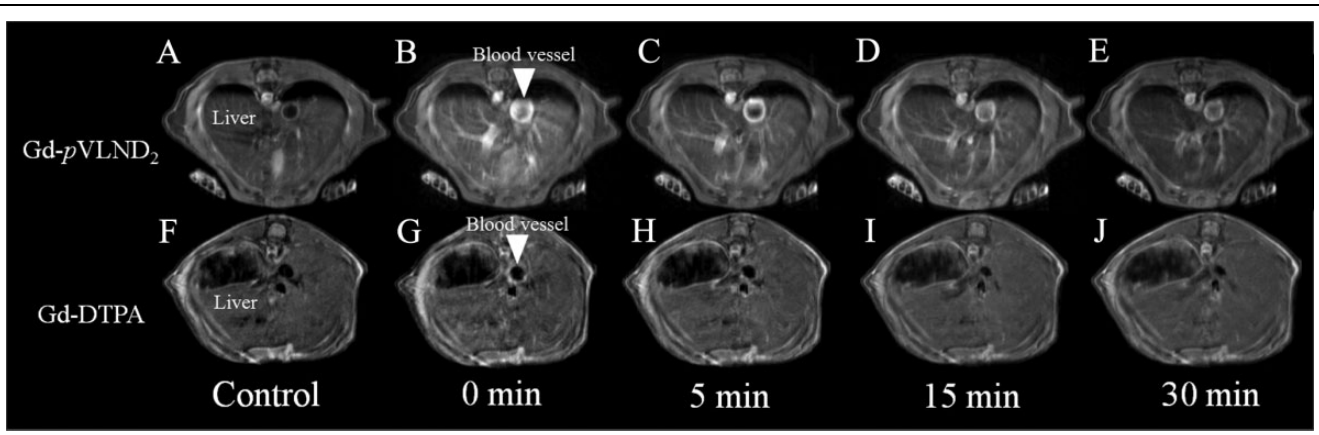

Figure 9. The MR images of normal ICR mice before (A) and after injection of Gd-pVLND$_2$ at 0 minutes (B), 5 minutes (C), 15 minutes (D), and 30 minutes (E); the MR images of normal ICR mice before (F) and after injection of Magnevist (Gd-DTPA) at 0 minutes (G), 5 minutes (H), 15 minutes (I), and 30 minutes (J). Gd indicates gadolinium, DTPA indicates diethylenetriaminepentaacetic acid; MR, magnetic resonance; pVLND$_2$, P(VLA-co-VNI-co-V$_2$DTPA).

accumulation of agents in the blood vessel. The higher blood uptake of Gd-pVLND$_2$ than that of ^{99m}Tc-Gd-pVLND$_2$ for SPECT imaging was due to the high injection dose for MR imaging. This is consistent with the blocking study in biodistribution or SPECT imaging, blocking with 200 μg GSA or cold copolymer leads to apparently increased blood uptake. For the clinical MR imaging contrast agent Magnevist, there have been no obvious enhancement of T_1 contrast in liver when the mouse was administrated with the same chemical quantity and concentration of Gd^{3+} as Gd-pVLND$_2$ (Figure 9F-J). The MR imaging results demonstrated that copolymer Gd-pVLND$_2$ had an obvious enhancement of T_1 contrast in vivo and specific liver targeting.

Conclusion

Copolymer pVLND$_2$ was successfully synthesized and could be labeled with radionuclide ^{99m}Tc and Gd simultaneously. The biodistribution study and SPECT imaging showed that it could target the liver specifically, and SPECT images had a high liver to background ratio. The different uptake results of the probe by normal and hepatic fibrosis mice afforded the potential to diagnose some hepatic disease. The MR imaging studies identified the multifunctional ability of the probe for multimodal imaging. Based on the copolymerization synthesis method, we believe that the sensitivity for MR imaging of the probe can be improved by adjusting the monomer ratio to increase the content of monomer V$_2$DTPA for Gd labeling. The design and synthesis method presented in this study provide useful strategies for other multifunctional imaging agents with different target molecule.

Acknowledgments

We thank Mr Jianbo Cao for helping with MR imaging.

Declaration of Conflicting Interests

The author(s) declared no potential conflicts of interest with respect to the research, authorship, and/or publication of this article.

Funding

The author(s) disclosed receipt of the following financial support for the research, authorship, and/or publication of this article: This study was financially supported by the National Natural Science Foundation of China (21271030, 81471707) and National Key Basic Research Program of China (2014CB744503).

Supplemental Material

The online [appendices/data supplements/etc] are available at http://mix.sagepub.com/supplemental.

References

1. Weber DA, Ivanovic M, Franceschi D, et al. Pinhole SPECT: an approach to in vivo high resolution SPECT imaging in small laboratory animals. *J Nucl Med*. 1994;35(2):342-348.
2. Roach PJS, Schembri GP, Ho Shon IA, et al. SPECT/CT imaging using a spiral CT scanner for anatomical localization: impact on diagnostic accuracy and reporter confidence in clinical practice. *Nucl Med Commun*. 2006;27(12):977-987.
3. Cherry SR. Multimodality *in vivo* imaging systems: twice the power or double the trouble? *Ann Rev Biomed Eng*. 2006;8:35-62.
4. Jennings LE, Long NJ. Two is better than one'—probes for dual-modality molecular imaging. *Chem Commun (Camb)*. 2009;(24):3511-3524.
5. Lee DE, Koo H, Sun IC, Ryu JH, Kim K, Kwon IC. Multifunctional nanoparticles for multimodal imaging and theragnosis. *Chem Soc Rev*. 2012;41(7):2656-2672.
6. Lee HY, Li Z, Chen K, et al. PET/MRI dual-modality tumor imaging using arginine-glycine-aspartic (RGD)–conjugated radiolabeled iron oxide nanoparticles. *J Nucl Med*. 2008;49(8):1371-1379.
7. Hu H, Huang P, Weiss OJ, et al. PET and NIR optical imaging using self-illuminating ^{64}Cu-doped chelator-free gold nanoclusters. *Biomaterials*. 2014;35(37):9868-9876.
8. Zhou J, Yu M, Sun Y, et al. Fluorine-18-labeled $Gd^{3+}/Yb^{3+}/Er^{3+}$ co-doped $NaYF_4$ nanophosphors for multimodality PET/MR/UCL imaging. *Biomaterials*. 2011;32(4):1148-1156.
9. Lewinski N, Colvin V, Drezek R. Cytotoxicity of nanoparticles. *Small*. 2008;4(1):26-49.
10. Lu ZR, Ye F, Vaidya A. Polymer platforms for drug delivery and biomedical imaging. *J Control Release*. 2007;122(3):269-277.
11. Ashwell G, Morell AG. The role of surface carbohydrates in the hepatic recognition and transport of circulating glycoproteins. *Adv Enzymol Relat Areas Mol Bio*. 1974;41(0):99-128.
12. Ashwell G, Harford J. Carbohydrate-specific receptors of the liver. *Ann Rev Biochem*. 1982;51(1):531-554.
13. Drickamer K. Ca (2+)-dependent sugar recognition by animal lectins. *Biochem Soc Trans*. 1996;24(1):146-150.
14. Pricer WE Jr, Hudgin RL, Ashwell G, Stockert RJ, Morell AG. A membrane receptor protein for asialoglycoproteins. *Methods Enzymol*. 1974;34:688-691.
15. Spiess M. The asialoglycoprotein receptor: a model for endocytic transport receptors. *Biochemistry*. 1990;29(43):10009-10018.
16. Stockert RJ. The asialoglycoprotein receptor: relationships between structure, function, and expression. *Physiol Rev*. 1995;75(3):591-609.
17. Löhr H, Treichel U, Poralla T, et al. The human hepatic asialoglycoprotein receptor is a target antigen for liver-infiltrating T cells in autoimmune chronic active hepatitis and primary biliary cirrhosis. *Hepatology*. 1990;12(6):1314-1320.
18. Jeong JM, Hong MK, Lee J, et al. ^{99m}Tc-neolactosylated human serum albumin for imaging the hepatic asialoglycoprotein receptor. *Bioconjug Chem*. 2004;15(4):850-855.
19. Yang W, Zhao Z, Fang W, Zhang X. The preparation of ^{99m}Tc-DTPA–LSA and its instant lyophilized kit for hepatic receptor imaging. *Appl Radiat Isot*. 2013;74(1):1-5.
20. Kudo M, Vera DR, Trudeau WL, Stadalnik RC. Validation of *in vivo* receptor measurements via *in vitro* radioassay: technetium-99m-galactosyl-neoglycoalbumin as prototype model. *J Nucl Med*. 1991;32(6):1177-1182.
21. Vera DR, Stadalnik RC, Trudeau WL, Scheibe PO, Krohn KA. Measurement of receptor concentration and forward-binding rate constant via radiopharmacokinetic modeling of technetium-99m-galactosyl-neoglycoalbumin. *J Nucl Med*. 1991;32(6):1169-1176.
22. Yang W, Mou T, Zhang X, Wang X. Synthesis and biological evaluation of ^{99m}Tc-DMP-NGA as a novel hepatic asialoglycoprotein receptor imaging agent. *Appl Radiat Isot*. 2010;68(1):105-109.
23. Yang W, Mou T, Guo W, et al. Fluorine-18 labeled galactosylated chitosan for asialoglycoprotein-receptor-mediated hepatocyte imaging. *Bioorg Med Chem Lett*. 2010;20(16):4840-4844.
24. Hwang EH, Taki J, Shuke N, et al. Preoperative assessment of residual hepatic functional reserve using ^{99m}Tc-DTPA-galactosyl-human serum albumin dynamic SPECT. *J Nucl Med*. 1999;40(10):1644-1651.
25. Liu C, Guo Z, Zhang P, et al. Kit formulated asialoglycoprotein receptor targeting tracer based on copolymer for liver SPECT imaging. *Nucl Med Biol*. 2014;41(7):587-593.
26. Yang W, Mou T, Shao G, Wang F, Zhang X, Liu B. Copolymer-based hepatocyte asialoglycoprotein receptor targeting agent for SPECT. *J Nucl Med*. 2011;52(6):978-985.
27. Kobayashi K, Sumitomo H, Ina Y. A carbohydrate-containing synthetic polymer obtained from Np-vinylbenzyl-D-gluconamide. *Polymer J*. 1983;15(9):667-671.
28. Markovsky E, Baabur-Cohen H, Eldar-Boock A, et al. Administration, distribution, metabolism and elimination of polymer therapeutics. *J Control Release*. 2012;161(2):446-460.
29. Liu T, Choi H, Zhou R, Chen IW. RES blockade: a strategy for boosting efficiency of nanoparticle drug. *Nano Today*. 2015;10(1):11-21.